ISSN (ONLINE): 2454-9762
ISSN (PRINT): 2454-9762
Available online at www.ijarmate.com

International Journal of Advanced Research in Management, Architecture, Technology and Engineering (IJARMATE)
Vol. 7, Issue 12,December 2021

3D Robust- brain tissue segmentation using MRI with weighted feature fusion

R.Punidha [1] , Professor
Department of Computer Science and Engineering
Bharathiyar Institute of Engineering for women
Thalaivasal , Salem

Alwar Rengarajan[2] , Professor
Department of Computer Science and Engineering
Bharathiyar Institute of Engineering for women
Thalaivasal , Salem

K Saranya[3] Assistant Professor
Department of Computer Science and Engineering
Bharathiyar Institute of Engineering for women
Thalaivasal , Salem

ABSTRACT- **Correct cell segmentation in brain magnetic resonance images is crucial during both mind restoration and evaluation. Super voxel analysis offers reasonably accurate segmentation of brain tissues by assigning 3D objects to tissue clusters based on the inherent knowledge of various features obtained first from issuing. Poor feature selection, poor feature use, and sloppy supreme boundaries caused by noise all contribute to clustering difficulties in this widely used system. The authors suggest a weighted features fusion clustering segmentation method that divides a three-dimensional object into three tissues based on a reliable feature fused similarity matrix in order to address the aforementioned issues.. In order to fully capture the similarities of characteristics among the issuing, we build three complementary similarities matrix on the basis of various characteristics from three aspects, namely appearance, shape, and spatial placement. The authors then propose a gives networking convnet to discriminatively combine the three similar matrices into a single layer. This innovative fusion process extracts the shared and statements that collectively perform of characteristics while also automatically adjusting the weight of commonalities based on their reliability. Finally, we achieve preliminary segmentation results by applying spectral clustering to the combined data matrix.. The separated boundaries affected by noise in the initial segmented images are optimised by the authors by taking into account the brightness information of adjacent voxels and creating a voxel-wise diffusion energy function. The efficacy of the proposed methodology was demonstrated through experiments using two publicly available brain magnetic resonance image datasets.**

Keyword: Magnetic Resonance Image, Segmentation, Supervoxel,

I INTRODUCTION

Grey matter (GM), white matter (WM), and cerebrospinal fluid (CSF) are separated from the magnetic resonance (MR) images of the brain using a process called tissue segmentation. For the construction, analysis, and understanding of the brain, segmentation is a crucial step [1-3]. Experts manually segment traditional brain MR images, which takes time and is inefficient when dealing with a large volume of brain MR images. Automatic segmentation in brain MR images has been proposed at this time. The images are typically two-dimensional (2D), with slices of the MRI images being displayed from top to bottom. In earlier methods, segmentation is done pixel-by-pixel. In recent years, it has been possible to combine the 2D brain image slices into a 3-dimensional (3D) image using complex computer calculations. Although the aforementioned methods could produce comparatively ideal segmentation results on a single slice, it is difficult to guarantee the continuity of tissues between adjacent slices given that they do not make use of 3D neighbouring information. Voxel-

ISSN (ONLINE): 2454-9762
ISSN (PRINT): 2454-9762
Available online at www.ijarmate.com

International Journal of Advanced Research in Management, Architecture, Technology and Engineering (IJARMATE)
Vol. 7, Issue 12,December 2021

wise segmentation, however, ignores spatial information and ineffectively makes use of regional image features. Furthermore, these techniques always involve a high computational cost due to the substantial number of voxels present in 3D MR images.

II METHODS

For noised brain MR images, we suggest a supervoxel-based weighted feature fusion clustering segmentation method (SWFFS). First, we create supervoxels using a well-known and traditional SLIC technique. Then, we determine each supervoxel's appearance, shape, and spatial location. We build the similarity matrices to gauge how similar each pair of supervoxels is based on the supervoxel-level features. The spectral clustering was then applied to the fused similarity matrix after we had combined these similarity matrices. Finally, using the information from nearby voxels, we create an energy function to smooth out the rough edges in the initial segmentation results.

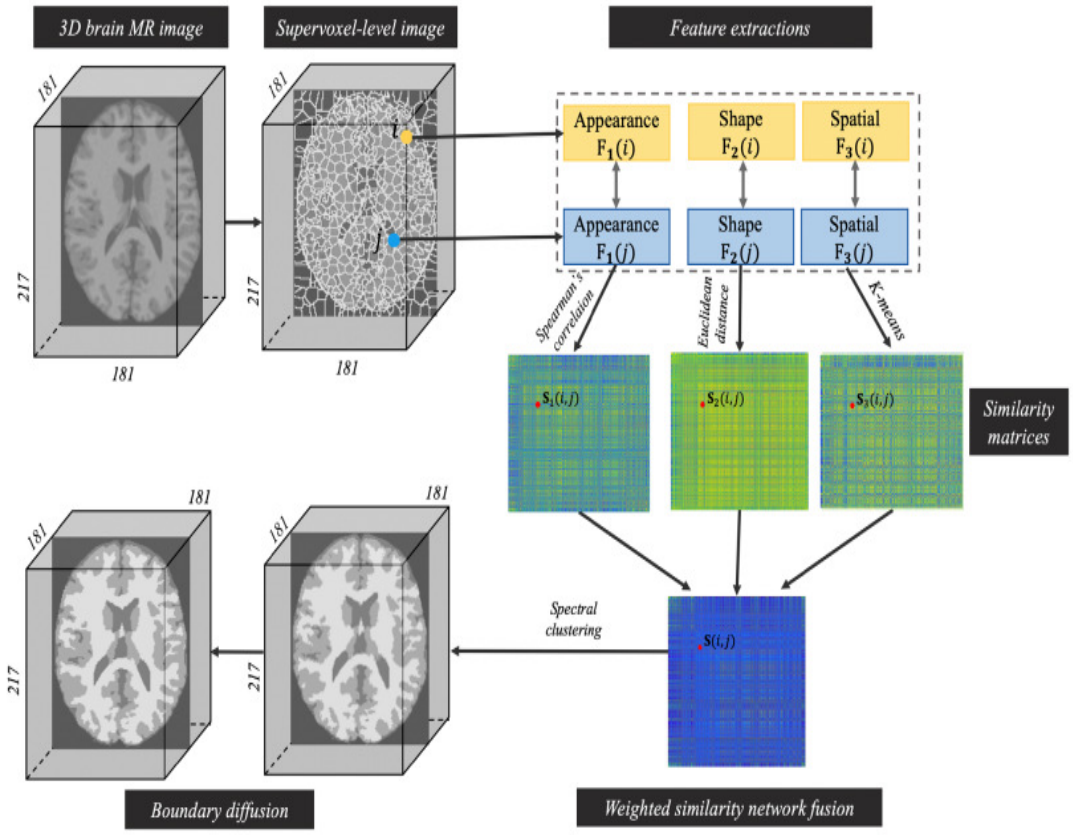

FIG 1: The framework of our segmentation method

III EXTRACTING SUPERVOXEL-LEVEL FEATURES

We first create the 3D supervoxels in brain MR images by using the SLIC algorithm, which is a modification of the k-means clustering approach, because our segmentation method operates at the supervoxel level. The number of supervoxels should be the only parameter that is specified in SLIC. SLIC handling 3D supervoxels requires consideration of the depth dimension to the spatial similarity term, in contrast to SLIC applied on 2D superpixel generation. In axial, sagittal, and coronal views, the supervoxels can adhere well to the boundaries between different tissues. This model is referred to as a

ISSN (ONLINE): 2454-9762
ISSN (PRINT): 2454-9762
Available online at www.ijarmate.com

International Journal of Advanced Research in Management, Architecture, Technology and Engineering (IJARMATE)
Vol. 7, Issue 12,December 2021

clustering model because each supervoxel is then assigned to the appropriate tissue category based on how similar its features are. The tissue segmentation results will be more accurate as more useful features are used in the clustering. It's anticipated that both broad and

specific information about supervoxels will be recorded.

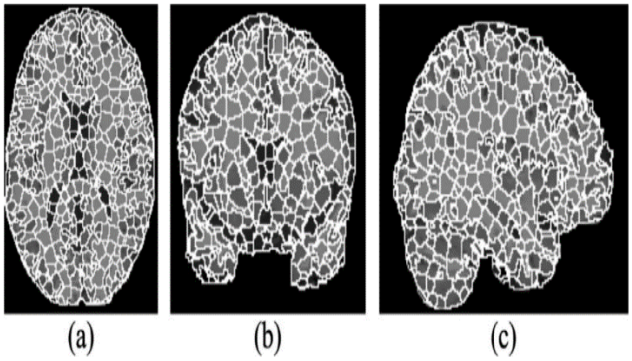

FIG 2: Super voxels generated by the SLIC algorithms.(a) Axial view, (b) sagittal view, and (c) Coronal view

IV CONSTRUCTING SIMILARITY MATRICES OF FEATURES

These features can be used to compare two supervoxels together in order to gauge how similar they are. We select the most appropriate similarity measurements for the various features of the brain tissues in order to accurately capture feature similarities among various supervoxels.

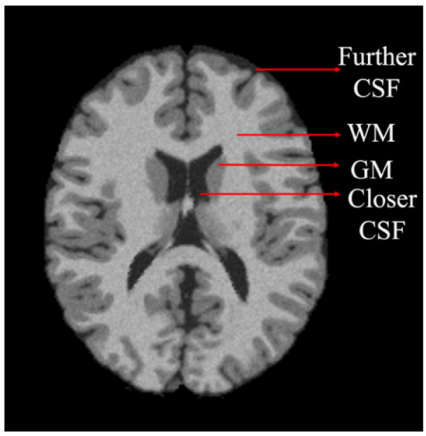

FIG 3: An example of different brain tissues

These features can be used to compare two supervoxels together in order to gauge how similar they are. We select the most appropriate similarity measurements for the various features of the brain tissues in order to accurately capture feature similarities among various supervoxels. In order to define the appearance feature F1, histograms, which display the intensity distribution of all the voxels within a supervoxel, are used. It is expected that the distributions of two histograms that are similar will be proportional or monotonic. The order of the elements affects the effectiveness of Spearman's correlation coefficient, which measures monotonic relationships. We determine the Spearman's correlation coefficient p between each pair of supervoxels I and j and determine how similar they are by comparing their visual characteristics:

$$S1(i, j) = 1 + p(F1(i), F1(j) 2 , i, j \in 1, .., N \quad (1)$$

The total number of supervoxels in this brain MR image is N. S1 is between 0 and 1. High correlation between two supervoxels suggests that their intensity histograms and intensity distribution are highly similar. Therefore, we use the straightforward Euclidean distance to compare the shape features of each pair of supervoxels. The Euclidean distance of the shape features F2(i) and F2(j) between each pair of supervoxels I and j is specifically denoted as dist(i, j), and the similarity S2 is defined as

$$S2(i, j) = 1 - dist(i, j) distmax , i, j \in 1, .., N. \quad (2)$$

The distmax in this case is the greatest dist among all supervoxels. S2 is between 0 and 1. High value between two supervoxels indicates that their key voxel intensities and boundary detail information are very similar. As a result, the distance between supervoxels I and j when they belong to the

ISSN (ONLINE): 2454-9762
ISSN (PRINT): 2454-9762
Available online at www.ijarmate.com

International Journal of Advanced Research in Management, Architecture, Technology and Engineering (IJARMATE)
Vol. 7, Issue 12,December 2021

same cluster is 0 (dist2(i, j)). Keep in mind that the clustering excludes the background. The final definition of the similarity between F3(i) and F3(j) is

$$S3(i, j) = 1 - dist2(i, j)\, dist2max\,,\ i, j \in 1, .., N. \quad (3)$$

The maximum dist2 among all supervoxels is represented here by dist2max. S3 has a range of 0 to 1. Close proximity to the central voxel is indicated by a high value between two supervoxels.

V ROBUST WEIGHTED SIMILARITY NETWORK FUSION

Clustering on the averaged matrix is a simple method for dividing the supervoxels into various tissue clusters in accordance with the complementary similarity matrices S1, S2, and S3. To be more precise, we first calculate a full kernel matrix P2 for each S2 as follows:

$$P2(i, j) = \begin{cases} w(i, j) \cdot S2(i, j) \\ \hline 2 \sum k \neq i\ w(i, k) \cdot S2(i, k)\,, & j \neq i \\ 1/2\,, & j = i\,; \end{cases} \quad (4)$$

$$w(i, j) = \begin{cases} 1 + \delta i \times \delta j\ /2(\delta i + \delta j)\,, \\ \text{if } i \leq \bar{\sigma} \text{ and } \sigma j \leq \bar{\sigma} \\ 1 - \delta i \times \delta j/\ 2(\delta i + \delta j)\,, \\ \text{if } \sigma i > \bar{\sigma} \text{ or } \sigma j > \bar{\sigma}\,, \quad j \neq i; \end{cases} \quad (5)$$

$$\delta i = \sigma i - \sigma min\ /\sigma max - \sigma min\ . \quad (6)$$

Here, σi is the supervoxel's voxel's intensity standard deviation. σmin, σmax and $\bar{\sigma}$ are the minimum, maximum and average standard deviations of all supervoxels, respectively. W is a robust weight that is calculated using the supervoxels I and j's standard deviation, which ranges from 0.80 to 1.30. Currently, the similarity of appearance and spatial features will aid in estimating the impact of noise on this supervoxel, and the other two full kernel matrices of appearance and spatial features are primarily responsible for the final fused similarity. In contrast, the intensities in supervoxels I and j are more homogeneous when their standard deviations are both lower than the average. In addition to ensuring that $\sum j\ Pm(i, j) = 1$, normalization also makes sure that P2 stays away from the self-similarity scale in the diagonal entries. P1 and P3 are defined as follows in light of the fact that S1 and S3 are largely unaffected by noise:

$$Pm(i, j) = \begin{cases} Sm(i, j)\ /2 \sum k \neq i\ Sm(i, k)\,, & j \neq i \\ 1/\ 2\,, \quad j = i \quad ; m \in \{1, 3\}. \end{cases} \quad (7)$$

Next, we compute the following sparse kernel matrix Qm:

$$Q\ m\ (i, j) \begin{cases} = Sm\ (i, j)/\ 2 \sum k \neq Ni\ Sm\ (i, k),\ j \neq Ni \\ 0, \quad \text{otherwise; } m \in \{1, 2, 3\}; \end{cases} \quad (8)$$

The neighbourhood of supervoxel i is represented by Ni, which stands for the K most similar supervoxels for supervoxel i. As a result, P1, P2 and P3 contain complete information about how each supervoxel compares to all other supervoxels based on features F1, F2, and F3, whereas Q1, Q2, and Q3 only contain information about how each supervoxel compares to the K most similar supervoxels. Pt m, m 1, 2, 3 is updated for iteration t in order to combine the three similarity matrices. $Pt\ m = Qm \times (\sum k \neq m\ Pt{-}1\ k\ 2) \times (Qm)\ T$,

$$m \in \{1, 2, 3\}. \quad (9)$$

The matrix transpose is represented here by () T. In Equations (8) and (9), the three matrices P1, P2, and P3 are combined using a message-passing method in which each iteration of the process results in a closer match between the three matrices. [2] discussed that Biomedical and anatomical data are made simple to acquire because of progress accomplished in computerizing picture division. More research and work on it has improved more viability to the extent the subject is concerned. A few techniques are utilized for therapeutic picture division, for example, Clustering strategies, Thresholding technique, Classifier, Region Growing, Deformable Model, Markov Random Model and so forth. This work has for the most part centered consideration around Clustering techniques, particularly k-implies what's more, fluffy c-implies grouping calculations. These calculations were joined together to concoct another technique called fluffy k-c-implies bunching calculation, which has a superior outcome as far as time usage. The calculations have been actualized and tried with Magnetic Resonance Image (MRI) pictures of Human cerebrum. The proposed strategy has expanded effectiveness and lessened emphasis when contrasted with different techniques. The nature of picture is assessed by figuring the proficiency as far as number of rounds and the time which the picture takes to make one emphasis. Results have been

ISSN (ONLINE): 2454-9762
ISSN (PRINT): 2454-9762
Available online at www.ijarmate.com

International Journal of Advanced Research in Management, Architecture, Technology and Engineering (IJARMATE)
Vol. 7, Issue 12,December 2021

dissected and recorded. Some different strategies were surveyed and favorable circumstances and hindrances have been expressed as special to each. Terms which need to do with picture division have been characterized nearby with other grouping strategies. [4] discussed about the combination of Graph cut liver segmentation and Fuzzy with MPSO tumor segmentation algorithms. The system determines the elapsed time for the segmentation process. The accuracy of the proposed system is higher than the existing system. The algorithm has been successfully tested in multiple images where it has performed very well, resulting in good segmentation. It has taken high computation time for the graph cut processing algorithm. In future work, we can reduce the computation time and improves segmentation accuracy.

VI CLUSTERING AND BOUNDARY DIFFUSION

We apply spectral clustering to the fused similarity matrix S to produce the initial segmentation results. Spectral clustering only uses the top eigenvectors in the similarity matrix's eigenspace in order to more accurately represent the point distributions of the input data. We set the number of clusters at 3, as spectral clustering requires a specific number of clusters. Some boundaries are affected by noise in the initial segmentation results because the SLIC method defines the boundary by using the intensity.

Combining the neighbourhood effect will aid in reducing the noise effect and correcting the supervoxel-based segmentation results. In the current study, we suggest a post-processing to soften the initial segmentation boundary that combines voxel-level neighbouring data with supervoxel-level information. Boundary diffusion is done on images that have been subjected to various levels of noise. The input image, the initial segmentation results, and the optimised segmentation results are shown in (a), (b), and (c), respectively. To reduce the noise or intensity, we specifically create a diffusion energy function that makes use of the neighbourhood information for each voxel.

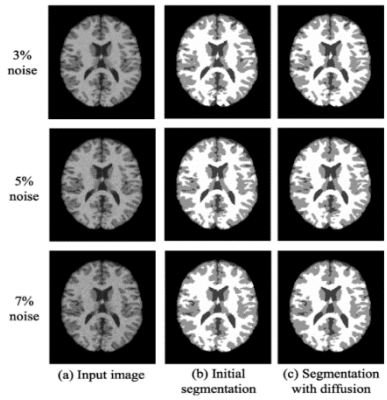

FIG 4: Boundary diffusion performed on images influenced by different levels of noises.

(a) Input image, (b) initial segmentation results, and (c) optimized segmentation results

In order to diffuse the boundaries in the initial segmentation results, the neighbouring information is iteratively combined by minimising the energy function. Following is a definition of the energy function:

E = I j, Ri, c(i), c(j), I M, v, vi, c(i), etc. (10)

The number of voxels in this MR image of the brain is M. Vi represents the voxel's intensity, Ri represents its spatial surroundings, and c(i) represents the cluster's centre intensity.

Each cluster's centre intensity is calculated as the sum of all the voxels in the cluster. The weight of nearby information is controlled by a smooth parameter called. To lessen the impact of noise, it can propagate the accurate cluster information from nearby voxels. To get the final segmentation result, the graph cuts method is used to solve the energy function in Equation (10). Some rough boundaries that were affected by noise are smoothed after this post-processing.

VII EXPERIMENTS

Two publicly accessible benchmark datasets are used in the current study to test the proposed segmentation algorithm. The first one is BrainWeb [29], which consists of six simulated brain MR volumes affected by various levels of noise and has a size of 181 217 181 voxels (https://brainweb.bic.mni.mcgill.ca). The second one is IBSR-18, which has a size of 256 x 256 x 128 voxels and contains 18 actual brain MR volumes. It can be found

ISSN (ONLINE): 2454-9762
ISSN (PRINT): 2454-9762
Available online at www.ijarmate.com

International Journal of Advanced Research in Management, Architecture, Technology and Engineering (IJARMATE)
Vol. 7, Issue 12,December 2021

at the Internet Brain Segmentation Repository (www.cma.mgh.harvard.edu/ibsr/).

All images come with their WM, GM, and CSF tissue ground truth segmentations. As shown in Figures 6 and 7, we rendered the WM and GM segmentation results' boundary to a 3D brain surface in order to visualise our 3D outcome. Sagittal and axial views of the surfaces are displayed. Particularly, as noise levels rise, segmentation results from FCM and FSL methods are more susceptible to noise influence, whereas SPM, RFCMSC, and SWFFS can produce segmentation results that are more reliable. especially in the areas close to the subcortex.

We use the segmentation accuracy (SA) to quantitatively evaluate the segmentation results. SA is defined as the ratio of correctly clustered voxels to the overall number of voxels. Formally,

$$SA = \sum C\ k=1\ Ak \cap Ck / \sum C\ i=1\ Ci. \qquad (11)$$

where Ak is the set of voxels belonging to the k class in the result, and Ck is the set of voxels belonging to the k class in the ground truth.

TABLE 1 Comparative SA analysis of different algorithms on brain web

Noise	Tissue	FCM	FSL	SPM	AWSFCM	RFCMSC	SWFFS
	WM	0.8126	0.7893	0.8876	0.9245	0.8903	0.9467
3%	GM	0.8377	0.7394	0.8992	0.8903	0.8857	0.9190
	CSF	0.9207	0.9305	0.9462	0.9483	0.9549	0.9680
	Total	0.9008	0.9031	0.9426	0.9511	0.9500	0.9671
	WM	0.8076	0.7533	0.8688	0.9235	0.8892	0.9371
5%	GM	0.8217	0.7356	0.8683	0.8864	0.8601	0.9038
	CSF	0.9070	0.9231	0.8985	0.9125	0.9254	0.9443
	Total	0.8952	0.8980	0.9365	0.9447	0.9398	0.9519
	WM	0.7912	0.7461	0.8554	0.9066	0.8675	0.9276
7%	GM	0.7909	0.7176	0.8595	0.8629	0.8437	0.8900
	CSF	0.8770	0.8971	0.8979	0.8954	0.8893	0.9228
	Total	0.8764	0.8719	0.9133	0.9290	0.9298	0.9354

ISSN (ONLINE): 2454-9762
ISSN (PRINT): 2454-9762
Available online at www.ijarmate.com

International Journal of Advanced Research in Management, Architecture, Technology and Engineering (IJARMATE)
Vol. 7, Issue 12,December 2021

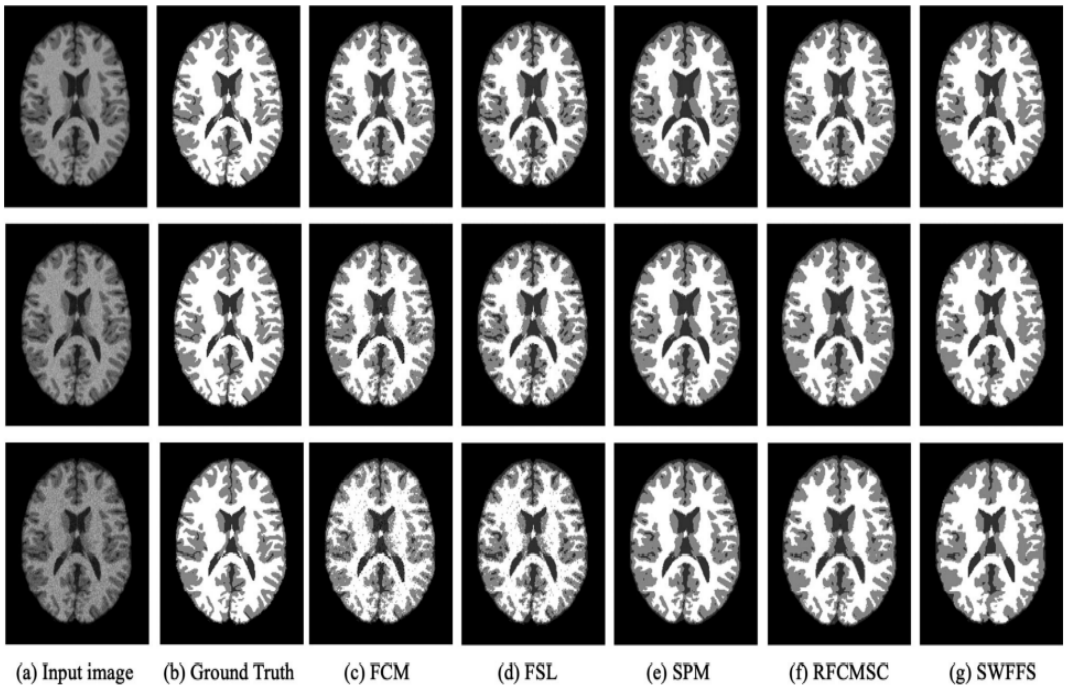

FIG 5: The segmentation results of brain MR images from Brain Web dataset with noise levels of 3%, 5% and 7% from up to bottom

VII REFERENCES

[1] Roy, S., Maji, P.: Rough segmentation of coherent local intensity for bias induced 3-D MR brain images. Pattern Recognit. 97, 106997 (2020)

[2]Christo Ananth, S.Aaron James, Anand Nayyar, S.Benjamin Arul, M.Jenish Dev, "Enhancing Segmentation Approaches from GC-OAAM and MTANN to FUZZY K-C-MEANS", Investigacion Clinica, Volume 59, No. 1, 2018,(129-138)

[3] Xia, J., Wang, F., Wu, Z., Wang, L., Zhang, C., Shen, D., et al.: Mapping hemispheric asymmetries of the macaque cerebral cortex during early brain development. Hum. Brain Mapp. 41(1), 95–106 (2020)

[4] Christo Ananth, D.R.Denslin Brabin, "ENHANCING SEGMENTATION APPROACHES FROM FUZZY K-C-MEANS TO FUZZY-MPSO BASED LIVER TUMOR SEGMENTATION", Agrociencia, Volume 54, No. 2, 2020,(72-84).

[5] Erdil, E., Ghani, M.U., Rada, L., Argunsah, A.O., Unay, D., Tasdizen, T., et al.: Nonparametric joint shape and feature priors for image segmentation. IEEE Trans. Image Process. 26(11), 5312–5323 (2017).

[6] Moyà Alcover, G., Elgammal, A., Jaume-i Capó, A., Varona, J.: Modeling depth for nonparametric foreground segmentation using RGBD devices. Pattern Recognit. Lett. 96, 76–85 (2017)

[7] Prakash, R.M., Kumari, R.S.S.: Spatial fuzzy c means and expectation maximization algorithms with bias correction for segmentation of MR brain images. J. Med. Syst. 41(1), 1–9 (2017)

ISSN (ONLINE): 2454-9762
ISSN (PRINT): 2454-9762
Available online at www.ijarmate.com

International Journal of Advanced Research in Management, Architecture, Technology and Engineering (IJARMATE)
Vol. 7, Issue 12,December 2021

[8] Wang, L., Nie, D., Li, G., Puybareau, É., Dolz, J., Zhang, Q., et al.: Benchmark on automatic six-month-old infant brain segmentation algorithms: The iseg-2017 challenge. IEEE Trans. Med. Imaging 38(9), 2219–2230 (2019)

[9] Kong, Y., Wu, J., Yang, G., Zuo, Y., Chen, Y., Shu, H., et al.: Iterative spatial fuzzy clustering for 3D brain magnetic resonance image supervoxel segmentation. J. Neurosci. Methods 311, 17–27 (2019)

[10] Wang, M., Liu, X., Gao, Y., Ma, X., Soomro, N.Q.: Superpixel segmentation: A benchmark. Signal Process. Image Commun. 56, 28–39 (2017)

[11] Xu, C., Corso, J.J.: Libsvx: A supervoxel library and benchmark for early video processing. Int. J. Comput. Vision 119(3), 272–290 (2016)

[12] Zhu, Z., Zheng, M., Qi, G., Wang, D., Xiang, Y.: A phase congruency and local Laplacian energy based multi-modality medical image fusion method in NSCT domain. IEEE Access 7, 20811–20824 (2019)

[13] Xia, J., Wang, F., Meng, Y., Wu, Z., Wang, L., Lin, W., et al.: A computational method for longitudinal mapping of orientation-specific expansion of cortical surface in infants. Med. Image Anal. 49, 46–59 (2018)